

Microstructure evolution, magnetic and mechanical properties of FePt/B₄C multifunctional multilayer composite films

Fujun Yang¹, Hao Wang¹, Hanbin Wang¹, Xin Cao¹,
Changping Yang¹, Quan Li², Mingjie Zhou², Yat-Ming Chong³
and Wen-Jun Zhang³

¹ Faculty of Physics and Electronic Technology, Hubei University, Wuhan 430062, People's Republic of China

² Department of Physics, The Chinese University of Hong Kong, Hong Kong, People's Republic of China

³ Department of Physics, City University of Hong Kong, NT, Hong Kong, People's Republic of China

E-mail: nanoguy@126.com (Hao Wang) and liquan@sun1.phys.cuhk.edu.hk (Quan Li)

Received 11 June 2007, in final form 4 September 2007

Published 19 October 2007

Online at stacks.iop.org/JPhysD/40/6735

Abstract

FePt/B₄C multilayer composite films with a Fe/Pt two-layer structure and a Fe/Pt/Fe sandwich structure were prepared by magnetron sputtering and subsequent annealing in vacuum. When the B₄C interlayer thickness of the FePt/B₄C films is bigger than 3 nm, a stable value of grain size, coercivity and hardness is observed. The characterizations of the microstructure demonstrate that the diffusion of B and C atoms in the FePt layer is so finite that the multilayer structure of the FePt/B₄C films is maintained after annealing at 500 °C for 30 min. The finite diffusion of B and C atoms is responsible for the FePt grain growth confinement, grain and layer separation and eventually induces the stable value mentioned above. The single composite films may find application in substituting the traditional three-layer structure commonly used in the present data storage technology.

(Some figures in this article are in colour only in the electronic version)

1. Introduction

The current thin film medium for magnetic recording applications usually employs a multilayer structure [1], i.e. a magnetic layer covered by additional protection layers and then suitable lubricants. L₁₀-ordered FePt films may be used as a magnetic layer due to their high magnetization (1100 emu cm⁻³) and large anisotropy ($K_u > 5 \times 10^7$ erg cm⁻³) [2]. Then the protection layer and the lubricant layer are added, which have good mechanical properties and lubricant properties. However, the grain size of pure FePt films is usually large and exchange coupling between the neighbouring grains cannot be weakened effectively. The requirement of a small particle size and reduced exchange

coupling among the particles can be satisfied by growing the FePt nanoparticles in a nonmagnetic matrix [3]. Previous works include employing FePt nanoparticles in B [4, 5], C [6, 7], B₂O₃ [8, 9], MgO [10], Al₂O₃ [11], FeMn [12], Ni [13], Mn [14], Ag [15, 16] and Cu [17, 18] matrices.

However, most studies only focused on the evolution of magnetic properties as a function of the FePt composition and grain size. There has been no systematic study exploring the use of single coatings that integrate multiple functions, namely, satisfactory mechanical, tribological and magnetic properties. In this study, we focus our research on multifunctional FePt/B₄C multilayer structures for ultra-high-density magnetic recording. The requirement of a small particle size and reduced exchange coupling among the particles can be satisfied by

introducing the B₄C nonmagnetic matrix. B₄C is the third hardest material after diamond and cubic boron nitride at room temperature. Moreover, the B₄C surface can be easily oxidized to boron oxide, which naturally absorbs water vapour in the air and forms boric acid, which is an excellent solid lubricant [19]. Therefore, the multifunctional film can provide all appropriate magnetic, mechanical and tribological properties required for ultra-high-density magnetic recording. Furthermore, the study can result in the further understanding of the evolution of various properties as a function of the B₄C interlayer thickness and the structure of the FePt magnetic layer.

2. Experiments

The [B₄C 12 nm]/[FePt 9 nm/B₄C x nm]₆ ($x = 0-7$ nm) multilayer precursors were deposited by magnetron sputtering on Si (001) substrates. Three 2.5 inch targets (B₄C 99.5%, Fe 99.9%, Pt 99.9%, Kurt J. Company) were used as the source material, and the multilayer thin films were deposited by rotating the substrate to the three targets successively. The FePt magnetic layers were obtained with a Fe/Pt two-layer structure and a Fe/Pt/Fe sandwich structure to discern the influence of different structures on properties. In order to protect the FePt layer from oxidation, the (6 - x) nm B₄C films are deposited subsequently when the thickness of the B₄C interlayer is less than 6 nm. During deposition, no substrate heating was applied. Then the as-deposited films were annealed in vacuum ($\sim 10^{-4}$ Pa) for 30 min.

The composition and thickness of the films were determined by x-ray photoelectron spectroscopy (XPS, PHI, Quantum 2000). The crystallinity and microstructure of the films were characterized by x-ray diffraction (XRD, Bruker D5) with CuK _{α} radiation and transmission electron microscope (TEM, Tecnai G2 FEG). The dark-field images were taken by a high-angle annular dark-field (HAADF) detector. Both energy dispersive x-ray spectrometer (EDS, EDX) and electron energy loss spectrometer (EELS, GIF) attached to the same microscope were used to obtain the compositional scanning profiles of the multilayer films. Room-temperature magnetic characteristics and exchange coupling were carried out by a vibrating sample magnetometer (VSM, Nanjing University Instruments HH 15 and Lakeshore 7407). The hardness and elastic modulus were measured using a Hysitron nanoindenter.

3. Results and discussion

The low magnification cross-sectional TEM images and corresponding high-resolution TEM images of composite Fe/Pt/Fe/B₄C films with different B₄C interlayer thicknesses annealed at 500 °C for 30 min are shown in figures 1 and 2. When the B₄C interlayer thickness is only 1 and 2 nm (figures 1(a) and (b)), the multilayer structure is barely discernible and no clear separation between the metal layers is observed in many regions of the films. Figures 2(a) and (b) show the corresponding high-resolution TEM images; as can be seen, the interface in between the B₄C and FePt layers of both samples is not smooth, and an interfacial roughness of ≈ 1 nm can be estimated. It is attributed to the intermixing of compositional elements in the multilayer films. Such intermixing first takes place during the deposition

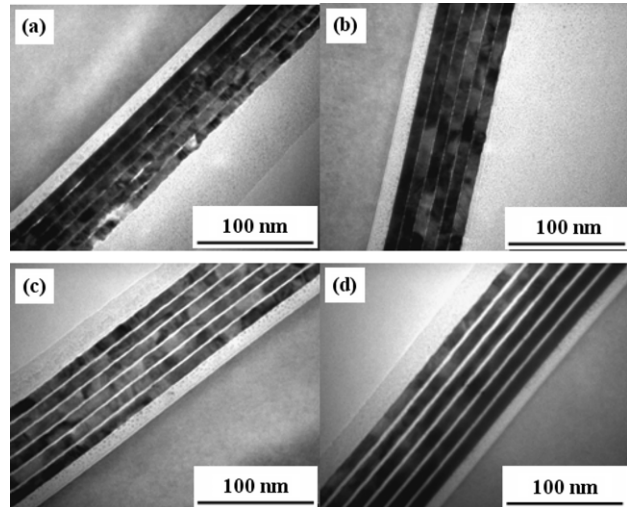


Figure 1. Low magnification cross section TEM images for (a) [Fe/Pt/Fe/B₄C 1 nm]₆ film, (b) [Fe/Pt/Fe/B₄C 2 nm]₆ film, (c) [Fe/Pt/Fe/B₄C 4 nm]₆ film and (d) [Fe/Pt/Fe/B₄C 6 nm]₆ film annealed at 500 °C for 30 min.

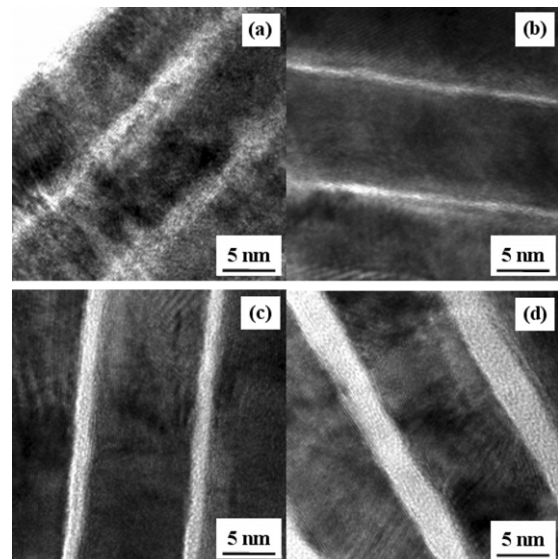


Figure 2. The high-resolution TEM images for (a) [Fe/Pt/Fe/B₄C 1 nm]₆ film, (b) [Fe/Pt/Fe/B₄C 2 nm]₆ film, (c) [Fe/Pt/Fe/B₄C 4 nm]₆ film and (d) [Fe/Pt/Fe/B₄C 6 nm]₆ film annealed at 500 °C for 30 min.

process—the island growth mode of the multilayer films results in incomplete separation between individual metallic layers at a small B₄C layer thickness. The incomplete separation makes it easy for the Fe and Pt atoms to diffuse among the multilayers in the post annealing process and leads to a ‘fused’ multilayer configuration. As the thickness of the B₄C interlayer is increased to 4 and 6 nm, a distinct multilayer configuration can be observed by TEM (figures 1(c) and 1(d)). It means thick B₄C interlayers effectively serve as spacers to separate the FePt layers, making the multilayer configuration stable even after annealing. The results suggest that the intermixing between FePt and B₄C layers has occurred after annealing, but the diffusion of compositional atoms is finite which is different from employing FePt nanoparticles in most of the reported matrices such as B [4, 5], C [6, 7] and B₂O₃ [8, 9]. Although

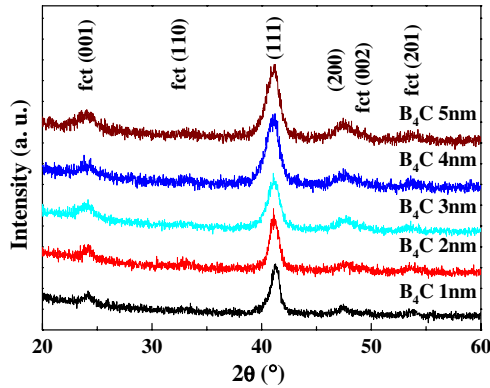


Figure 3. XRD patterns of Fe/Pt/Fe/B₄C films with different B₄C interlayer thicknesses annealed at 500 °C for 30 min.

there should also exist B and C atoms in the FePt layer, no concentrated white regions are discernible in figures 2(c) and 2(d). It is likely due to the average distribution and the finite number of B and C atoms in the FePt layer. In the corresponding compositional line scanning profile which is not shown here, signals from B and C atoms are detectable even in the interior of the FePt layer; however, the Fe and Pt signals are mainly restricted to the FePt layers and the interfacial region (given that the interfacial roughness is about 1 nm). This is due to the small atomic radius of B and C atoms and the polycrystalline nature of the FePt layer, leading to their diffusion being easy than Fe and Pt.

It is known that two kinds of phases, namely, face centred-cubic (fcc) and face-centred-tetragonal (fct) phases, exist in the FePt alloy while only the fct phase has a large K_u value. Figure 3 shows the XRD patterns of Fe/Pt/Fe/B₄C films with a different B₄C interlayer thickness annealed at 500 °C for 30 min. A superlattice (001) peak is observed in all samples which means the existence of part phase transformation. As the B₄C interlayer thickness increases from 1 to 2 nm, the appearance of the superlattice (110) peak and the intensity improvement of the fct (001) peak indicate a more complete phase transformation. So the addition of the B₄C layers can enhance the phase transformation of the Fe/Pt/Fe/B₄C films. Further increasing the B₄C interlayer thickness to over 3 nm, the (111) peak is broadened obviously which means the decrease in the FePt grain size.

The FePt grain sizes of the FePt/B₄C composite films with a Fe/Pt two-layer structure and a Fe/Pt/Fe sandwich structure are estimated using the (111) peak in the XRD spectrums based on the Scherrer formula. Figure 4 shows the FePt grain size of the composite Fe/Pt/B₄C and Fe/Pt/Fe/B₄C films changing with the B₄C interlayer thickness. The grain size of the Fe/Pt/Fe/B₄C films shows a trivial decrease after increasing the B₄C interlayer thickness from 1 to 2 nm. It is ascribed to that the B and C atoms are mainly restricted to the B₄C interlayers and that the diffusion of B and C atoms is finite. As the thickness of the B₄C interlayer is increased to 3 nm, the grain size decreases to ~6.25 nm. It is attributed to the increasing diffusion of B and C atoms which suppresses the grain growth of FePt grains. Nevertheless, a further increase in the B₄C interlayer thickness (>3 nm) seems to have little effect on promoting the diffusion of B and C atoms into the FePt layer, thus further decreasing the FePt grain size. It is

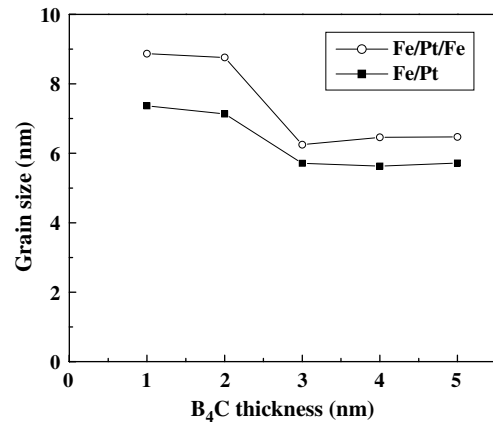


Figure 4. The FePt grain size of the composite Fe/Pt/B₄C and Fe/Pt/Fe/B₄C films changing with the B₄C interlayer thickness.

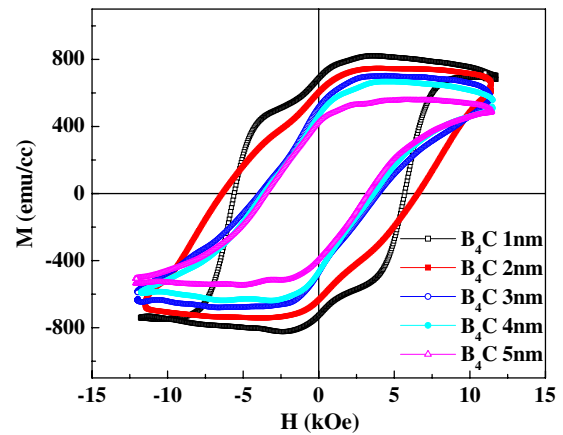


Figure 5. In-plane magnetization curves of the composite Fe/Pt/Fe/B₄C films annealed at 500 °C for 30 min with different B₄C interlayer thicknesses.

due to the saturation of the diffusion of B and C atoms, i.e. the further increase in the B₄C interlayer thickness will cause little change in the number of B and C atoms in the FePt layer. In Fe/Pt/B₄C films, the grain size has the same changing tendency as that in Fe/Pt/Fe/B₄C films, in which the thick Fe layer is divided into two layers and the thin Pt layer is contained between them. It means the formation of the thick FePt magnetic layer is much more convenient in Fe/Pt/Fe/B₄C films than in Fe/Pt/B₄C films, which induces larger FePt grains.

The magnetic properties of the composite films have a strong dependence on the B₄C interlayer thickness. In-plane magnetic hysteresis loops of Fe/Pt/Fe/B₄C films annealed at 500 °C for 30 min with different B₄C interlayer thicknesses are shown in figure 5. As the B₄C interlayer thickness increases from 1 to 2 nm, the coercivity increases from 5.58 to 6.47 kOe. The improvement in coercivity can be ascribed to (i) the better confinement of Fe atoms in the FePt layer, which leads to more stoichiometric FePt and thus higher coercivity and (ii) the complete separation of the FePt layer as well as the B and C atoms in the FePt layer contributes to the isolation of the FePt grains, leading to the weakened exchange coupling in the composite film. Further increase in the B₄C

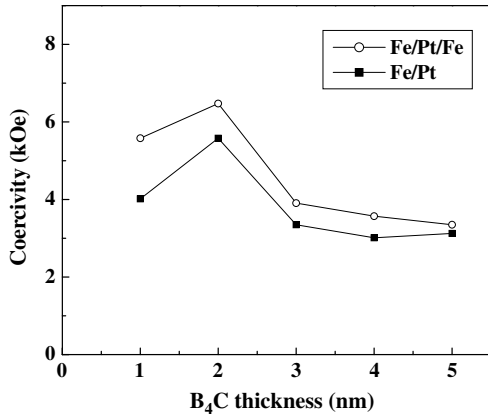


Figure 6. Plot of coercivity of the composite Fe/Pt/B₄C and Fe/Pt/Fe/B₄C films changing as a function of the B₄C interlayer thickness.

interlayer thickness to 3 nm results in the coercivity decreasing to 3.91 kOe. The decrease is attributed to the diffusion of more B and C atoms into the FePt layer which suppresses the grain growth of FePt grains. As the B₄C interlayer thickness is above 3 nm, the intermixing will not increase with the increase in the B₄C interlayer. The saturation of diffusion of B and C atoms induces a stable value of coercivity.

The magnetic properties of FePt/B₄C films also have a strong dependence on the structure of the FePt magnetic layer. Figure 6 plots the coercivities of the FePt/B₄C composite films with a Fe/Pt two-layer and a Fe/Pt/Fe sandwich structure as a function of the B₄C interlayer thicknesses. In the Fe/Pt/B₄C composite films, the magnetic property is also influenced by the intermixing of the compositional atoms. The coercivity value of the Fe/Pt/B₄C films has the same changing tendency as that of the Fe/Pt/Fe/B₄C films. But the value is less than that of the Fe/Pt/Fe/B₄C films. It is caused by a smaller FePt grain size of the Fe/Pt/B₄C films than that of the Fe/Pt/Fe/B₄C films (as discussed in figure 4).

The Kelly–Henkel plot (also called the δM plot) has been proposed as means of estimating the amount of intergranular exchange present in thin film recording media [20]:

$$\delta M(H) = M_d(H)/M_s - [1 - 2M_r(H)/M_s],$$

where $M_d(H)$ is the dc-demagnetization remanence (DCD) curve and $M_r(H)$ is the isothermal remanence (IRM) curve. Negative or positive deviation of δM means that the predominant intergranular interactions are dipolar or exchange coupled. Figure 7 shows the δM curves of [Fe/Pt/Fe/B₄C 1 nm]₆ and [Fe/Pt/Fe/B₄C 2 nm]₆ films. With increasing thickness of the B₄C interlayer from 1 to 2 nm, the positive peak in the δM plot becomes much weaker, suggesting that the exchange coupling is reduced rapidly. This is attributed to the diffusion of B and C atoms which affects the exchange interactions in two ways. One is the separation of both the FePt layer and the FePt grains by more B and C atoms, reducing the exchange (but not dipolar) interactions. Another is the decrease in the soft magnetic phase fraction (more stoichiometric FePt and more completed phase transformation as discussed above), reducing the exchange interaction between the soft and hard magnetic phases. It can be observed that the negative and positive deviations of

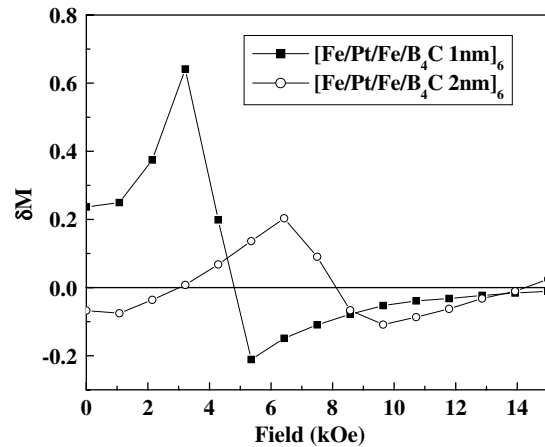


Figure 7. δM curves of [Fe/Pt/Fe/B₄C 1 nm]₆ and [Fe/Pt/Fe/B₄C 2 nm]₆ films annealed at 500 °C for 30 min.

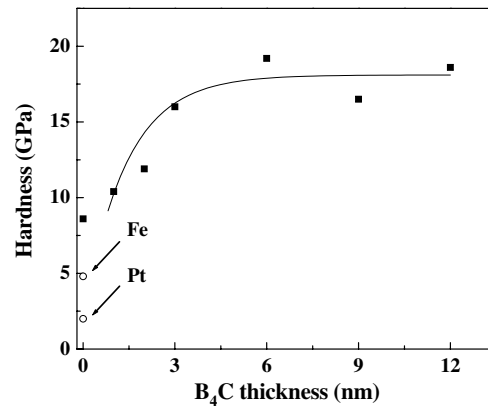


Figure 8. The hardness of the composite Fe/Pt/Fe/B₄C films annealed at 500 °C for 30 min as a function of the B₄C interlayer thickness.

δM of the [Fe/Pt/Fe/B₄C 2 nm]₆ sample were almost equal, which means the exchange coupling will be reduced with difficulty even increasing the thickness of the B₄C interlayer further. This is consistent with the aforementioned saturation of diffusion of B and C atoms.

The hardness of the diamond-like carbon protective coating (~5 nm) on commercial hard disc media is estimated to be about 20 GPa. But the overall value of hardness is far less than 10 GPa when the coating is measured with the media and the substrate. Figure 8 shows the hardness of the Fe/Pt/Fe/B₄C films as a function of the B₄C interlayer thickness. The hardness from a pure Fe and a pure Pt film are approximately 4.8 GPa and 2.0 GPa [21], respectively. This yields a rule of mixture value of 3.5 GPa for a pure FePt film. However, for the present FePt multilayers without B₄C layers, the hardness is about 8.5 GPa, which is about 2.4 times the value estimated by the rule of mixture. This hardness enhancement is due to the strengthening effect of the multilayer configuration which has been shown in the epitaxial Fe(0 0 1)/Pt(0 0 1) multilayers [21] and a number of other multilayer systems [22–24]. The value of hardness increases gradually to 10.4 GPa and then to 16 GPa with increasing B₄C interlayer thickness from 1 to 3 nm. Further increase in the B₄C interlayer thickness up to 12 nm has little impact on the hardness of the FePt/B₄C films which is

stable between 16 and 20 GPa. The measured hardness value is, in fact, much higher than that predicted by the rule of mixture and even higher than that after considering the strengthening effect of the multilayer configuration. Therefore, the hardness enhancement of the composite film upon the addition of the B₄C interlayer may not only be due to the intrinsic high hardness of B₄C and multilayer configuration but may also be induced by the diffusion of B and C atoms into FePt grain boundaries which act as obstacles to dislocation motion. The saturation of hardness is similar to that of grain size and coercivity which is also induced by the saturation of diffusion of B and C atoms.

4. Conclusion

On concluding, we find that FePt/B₄C multilayer composite films can have better magnetic properties by changing Fe/Pt to a Fe/Pt/Fe sandwich structure. The B₄C interlayer in the FePt/B₄C multilayer composite films has several effects on their structure and magnetic properties. The increase in the of B₄C interlayer thickness could suppress the grain growth and exchange coupling of FePt grains. The coercivity of FePt/B₄C films increases first and then decreases to a stable value with increasing B₄C interlayer thickness. By adopting a Fe/Pt/Fe sandwich structure and varying the thickness of the B₄C interlayer, a small grain size (8.76 nm), satisfactory coercivity (6.47 kOe), stable hardness (16–20 GPa) and low exchange coupling of FePt grains can be achieved. Finally, the three layer structures in magnetic recording media, i.e. a magnetic layer covered by additional protection layers and then suitable lubricants, may be substituted by single FePt/B₄C composite films.

Acknowledgments

The authors acknowledge the financial support from the National Nature Science Foundation of China under Grant No 50371056, the Natural Science Foundation Creative Team Project of Hubei Province (2007ABC005), the Excellent Yong Scientist Foundation of Hubei Province (2005ABB033) and the Research Grants Council of Hong Kong SAR (Ref. No. CUHK4182/04E).

References

- [1] Wang S X and Taratorin A M 1999 *Magnetic Information Storage Technology* (New York: Academic) chapter II
- [2] Weller D, Moser A, Folks L, Best M E, Lee W, Toney M F, Schwickert M, Thiele J U and Doerner M F 2000 *IEEE Trans. Magn.* **36** 10
- [3] Wang H and Wong S P 2002 *Magnetic Nanostructures* ed H S Nalwa (Stevenson Ranch, CA: American Scientific Publishers) p 407
- [4] Li N and Lairson B M 1999 *IEEE Trans. Magn.* **35** 1077
- [5] Aoyama T, Sato I, Ito H and Ishio S 2005 *J. Magn. Magn. Mater.* **287** 209
- [6] Perumal A, Ko H S and Shin S C 2003 *Appl. Phys. Lett.* **83** 3326
- [7] Chen J S, Ding Y F, Lim B C and Liu E J 2006 *IEEE. Trans. Magn.* **42** 2363
- [8] Luo C P, Liou S H, Gao L, Liu Y and Sellmyer D J 2000 *Appl. Phys. Lett.* **77** 2225
- [9] Yan M L, Zeng H, Powers N and Sellmyer D J 2002 *J. Appl. Phys.* **91** 8471
- [10] Kim H J and Lee S R 2005 *J. Appl. Phys.* **97** 10H304
- [11] White C W, Withrow S P, Williams J M, Budai J D, Meldrum A, Sorge K D, Thompson J R and Boatner L A 2004 *J. Appl. Phys.* **95** 8160
- [12] Phuoc N N and Suzuki T 2006 *J. Appl. Phys.* **99** 08C107
- [13] Yan M L, Xu Y F, Li X Z and Sellmyer D J 2005 *J. Appl. Phys.* **97** 10H309
- [14] Huang J C A, Chang Y C, Yu C C, Yao Y D, Hu Y M and Fu C M 2003 *J. Appl. Phys.* **93** 8173
- [15] Kang K, Zhang Z G, Papusoi C and Suzuki T 2003 *Appl. Phys. Lett.* **82** 3284
- [16] Zhou Y Z, Chen J S, Chow G M and Wang J P 2004 *J. Appl. Phys.* **95** 7495
- [17] Berry D C, Kim J, Barmak K, Wierman K, Svedberg E B and Howard J K 2005 *Scr. Mater.* **53** 423
- [18] Chen S K, Yuan F T and Chin T S 2005 *J. Appl. Phys.* **97** 073902
- [19] Erdemir A, Bindal C and Fenske G R 1996 *Appl. Phys. Lett.* **68** 1637
- [20] Kelly P E, Grady K O, Hayo P I and Chantrell R W 1989 *IEEE Trans. Magn.* **25** 3881
- [21] Daniels D J, Nix W D and Clemens B M 1995 *Appl. Phys. Lett.* **66** 2969
- [22] Chu X and Barnett S A 1995 *J. Appl. Phys.* **77** 4403
- [23] Yashar P, Barnetta S A, Rechnerb J and Sproulb W D 1998 *J. Vac. Sci. Technol.* **16** 2913
- [24] Martínez E, Romero J, Lousa A and Esteve J 2002 *J. Phys. D: Appl. Phys.* **35** 1880